Optical, Structural and Magnetic Characterization of Iron Oxide and Gold Core-Shell Nanoparticles Synthesized by Pulsed Laser Ablation in Liquid

Mustafa Jassim Ismael[1], Nadia Mohammed Jassim[2] and Wafaa Hameed Abbas[3]
[1]*Department of Physics, College of Science, University of Diyala, 32001 Baqubah, Iraq*
[2]*Department of Physics, College of Education for Pure Sciences, University of Diyala, 32001 Baqubah, Iraq*
[3]*Department of Studies, Planning and Follow-up, Ministry of Higher Education and Scientific Research, 10001 Baghdad, Iraq*
sciphyphd242505@uodiyala.edu.iq, nadiajassim@uodiyala.edu.iq, w.hameedabbas1983@edu.iq

Keywords: Fe_2O_3/Au Core-Shell, PLAL; SPR, Magnetic Properties, Gold Nanoparticle, Iron Oxide Nanoparticles.

Abstract: The composition nanoparticles of gold and iron oxide were produced in this study through laser ablation in liquid (PLAL) and analyzed with the help of various analytical methods. The X-ray diffraction (XRD) results revealed sharp peaks of gold with face-centered cubic crystal structure at the angles of 38.2, 44.4, 64.6, and 77.5 representing the sizes of the particles as nanoscale and quasi-crystalline. The results obtained indicated a crystal structure in gold which are sharp at angles of 38.2, 44.4, 64.6 and 77.5. The results of the energy-dispersive spectroscopy (EDS) analysis proved the purity of the sample with gold predominant in the proportion of weight (percentage 87.55) and atomic (percentage 66.59) percentage over iron. The optical absorption spectra exhibited hybridization between surface Plasmon resonance of gold and semiconducting characteristics of the iron oxide which is indicated by Tak diagram that had several energy gaps at 2.2-2.3 eV and 3.2-3.3 eV. The images (TEM) and (SEM) proved that a core-shell structure with an average particle size of 8.52 + 5.06 nm was successfully formed and that pyramidal clusters with an average size of 90.44 + 72.44 nm were present respectively. In general, the work showed how laser scraping technology was effective in making high levels of composite nanoparticles with an improved optical and magnetic characteristic that is applicable in bioenergy and energy.

1 INTRODUCTION

Gold nanoparticles (AuNPs) represent a type of nanomaterial that has been studied and utilized over the recent decades because of its distinctive physical and chemical characteristics. The particles have localized surface plasmon resonance (LSPR), which has provided them with outstanding optical characteristics that are extremely reliant on the size, the shape, and the surrounding medium and makes them more suitable in biosensing and medical imaging workloads [1]. Moreover, gold nanoparticles are highly biocompatible and can simply be chemically modified to conjugate biomolecules like antibodies and drugs extending their use to targeted diagnostics and therapy [2].

Conversely, iron oxide nanoparticles (IONPs) are of significant interest in biomedical application because of their outstanding magnetism characteristics especially the superparamagnetism which is realized at the nano scale. This enables them to react to external magnetic fields without being left with remains of magnetism once the field has been removed [3]. Iron oxides come in several crystalline forms with the most significant ones being magnetite (Fe_3O_4), magnetite (g-Fe_2O_3) and hematite (a-Fe_2O_3). Each of the three is low-toxic and biodegradable and thus has been approved by the US Food and Drug Administration (FDA) to be used in clinical applications, like contrast in magnetic resonance imaging (MRI) and magnetotherapy [4].

The introduction of these two materials into the core-shell composite nanoparticles (Fe_2O_3/Au), is a step forward in the creation of a composite nanoparticle that is a blend of the usefulness of both materials into a single material. The core in this structure is the source of magnetic properties, which make it possible to separate and orient the magnetic particles, and the shell of gold shell gives the core chemical stability against oxidation and corrosion as

well as plasmonic optical properties and readily modified with thiols [5]. This practical amalgamation produces theranostic materials that can diagnose and treat in the same time. Photothermal therapy can be performed using gold, and iron oxide in the case of a magnetic resonance imaging (MRI) [6]. The two materials selected in this study were chosen based on the complementarity of their properties. Iron provides structural support and important magnetic properties, while gold exhibits high chemical stability and advanced optical characteristics. Gold also displays surface plasmon resonance, which enhances its interaction with electromagnetic radiation and improves the system's optical response [7].

Furthermore, gold has superior oxidation resistance compared to alternative materials such as silver or copper, ensuring long-term performance stability. Although some of these materials may possess higher conductivity, their susceptibility to oxidation limits their efficiency, making gold a more suitable choice for balancing optical performance and stability [8].

The ways to prepare these composite particles are different and they include wet chemical methods, which include co-chemical reduction and sol-gel techniques. Nevertheless, laser ablation in liquid (LAL) has become a viable and green technique. This method consists of illuminating a solid target (an alloy or layers of iron and gold) which has been placed in a liquid with high-energy laser pulses. This forms a plasma, which condenses into pure nanoparticles without the use of reducing or stabilizing chemicals which may be toxic [9]. These ready particles have diverse applications, such as drug delivery to specific places, photothermal therapeutic use against cancer, photocatalysis, and very sensitive biosensors [10].

Lastly, a complex of experimental factors affects the charecteristics of the Fe_2O_3/Au composite particles prepared by laser ablation. These parameters are laser parameters that are wavelength, pulse duration (nanometers vs. femtoseconds), and laser energy (fluence) that dictates the particle size and crystalline distribution [11]. Furthermore, the nature of the liquid medium (water, ethanol, etc.) and the time of the skimming are important to the definition of surface chemistry and the state of the $_2$oxidation since the reaction between the plasma and the liquid molecules may result in the growth of oxide or carbon coating that determine the ultimate characteristics of the composite [12].

In this research, gold and iron oxide nanoparticles will be synthesized using LAL technique (Fig. 1). The optical and structural properties will be examined using UV spectrophotometer, TEM, FESEM and XRD spectroscopy.

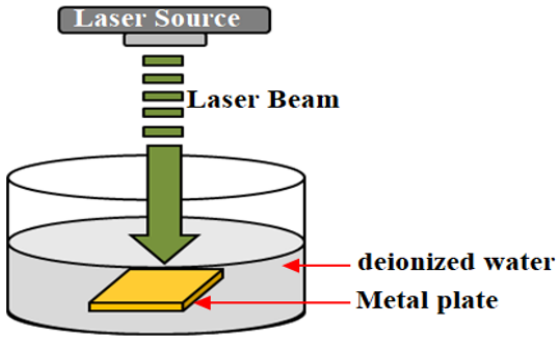

Figure 1: Laser ablation system.

2 MATERIAL AND METHOD

The Composite Fe_2O_3/Au core shell nanoparticles will be synthesized by pulsed laser ablation in liquid (PLAL) using pure metal targets of 99.9% iron and gold. The pure medium contained 10 mL of deionized water and each of the targets was placed in a glass cell separately. A Q-switched Nd:YAG pulsed laser (produced by HUAFEL, China) with two wavelengths (1064 and 532 nm) with a peak pulse energy of 1000 mJ, and pulse duration of 10ns was utilized. The laser used in this work was at a wavelength of 1064 nm pulse energy of 600 mJ, pulse width of 10 n and 500 pulses. The core-shell structure was attained with a given preparation procedure. To begin with, a sheet of pure gold was put in deionized water and ablated using laser to get the particles of gold that would constitute the shell. The cell was then emptied of the gold, and a sheet of pure iron was put into the solution to undergo the second ablation process to get the iron oxide core. This enabled Fe_2O_3/Au composite particles of the core-shell structure to be formed in the final colloidal suspension.

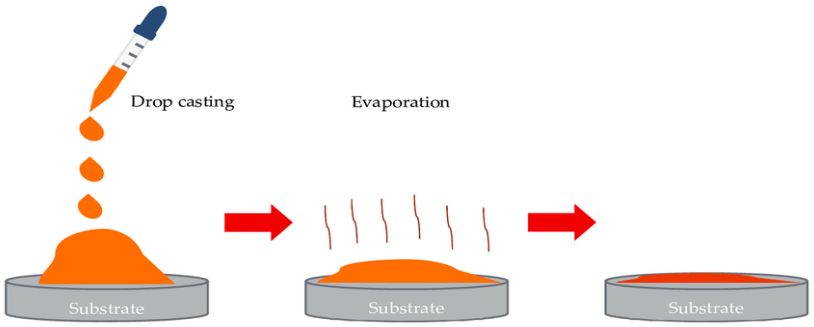

Figure 2: Drop-casting procedure.

When the ablation processes were accomplished and the colloidal suspension of the composite nanoparticles was obtained, the resulting solution was then deposited onto the quartz substrates with the help of drop casting to create uniform thin layers (Fig. 2).

3 RESULTS AND DISCUSSION

The X-ray diffraction (XRD) pattern of nanoparticles extracted by laser liquid deposition (PLAL) shows a broad, low-intensity peak in the (2θ=20–25°) range, this is because the extracted particles are within the Nano scale dimensions and the possibility of amorphous iron oxide within these nanoparticles (Fig. 3) [13]. Distinct sharp peaks are observed at approximate diffraction angles of 38.2, 44.4, 64.6, and 77.5°, with orientations (111), (200), (220), and (311) of face-centered cubic (FCC) gold, confirming the crystalline phase of gold [13]. The peak width is inversely proportional to the crystallite size; broader peaks indicate smaller crystal size. the crystallite was size estimated using the Shearer equation D= (Kλ)/(β COSθ), the average crystallite size was found to be approximately 9 nm, while the size calculated from the (111) plane was about 22nm [14]. In the case of iron oxide, broad peaks at low angles indicate the presence of a mixture of other iron oxide compounds, including magnetite (Fe_3O_4) and magnetite (Fe_2O_3). This is consistent with studies that found laser ablation produces multiple phases of iron oxide depending on the laser energy and the liquid medium used [15]. The absence of sharp peaks in iron oxide, which are easily visible, may be attributed to the size of the iron oxide nanoparticles or to the presence of a gold layer on the core-shell particles. In the latter case, only gold peaks appear in the X-ray diffraction spectrum because they have high diffraction
power [13].

Energy-dispersive X-ray spectroscopy (EDS) was also used for the elemental analysis of gold and iron oxide nanoparticles (Fig. 4). The results showed distinct spectral peaks for the target elements, with the emission peaks of iron (Fe) and gold (Au) clearly visible, specifically the Fe Lα line and the M (estimated at approximately 2.2 kV) and L (estimated at approximately 9.7 and 11.4 kV) emission series, respectively [13]. Quantitative data in the accompanying table show that gold is the predominant element in terms of weight percentage (W%), at 87.55%, compared to 12.45% for iron. This difference is primarily attributed to the significant difference in atomic mass between the two elements (gold is considerably heavier than iron). However, the atomic percentage (A%) is more homogeneous, at 66.59% for gold and 33.41% for iron. The absence of any other impurity peaks in the spectrum indicates the efficiency of laser ablation in producing high-purity nanomaterials without the reduction or stabilization of chemicals that may remain in their organic state. This is consistent with studies demonstrating the ability to prepare core-shell structures directly in a liquid medium [14], [16].

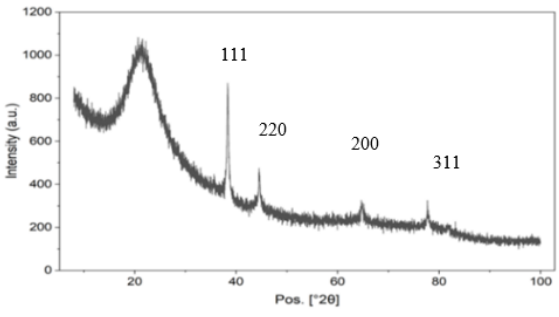

Figure 3: X-ray diffraction (XRD) pattern of Fe_2O_3/Au core-shell nanoparticles.

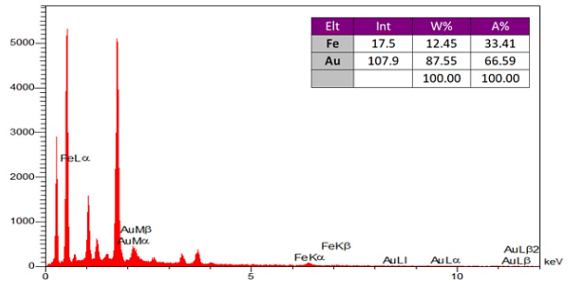

Figure 4: Energy-dispersive X-ray spectroscopy (EDS) of Fe_2O_3/Au core-shell nanoparticles.

Absorbance curve versus wavelength displays the high UV absorbance which decreases slowly throughout the visible spectrum, reaching the infrared (Fig. 5). The principal Tauc plot is a representation of the relationship between $(\alpha h\nu)^2$ and the energy of photons, which shows several electronic transitions at the various values of energy, with crossovers to the energy axis showing several optical energy gaps. The largest minimum energy gap value (around 2.2 -2.3 eV) is that of the direct energy gap of alpha-Fe_2O_3 or it varies according to the level of crystallinity and mode of preparation [13].

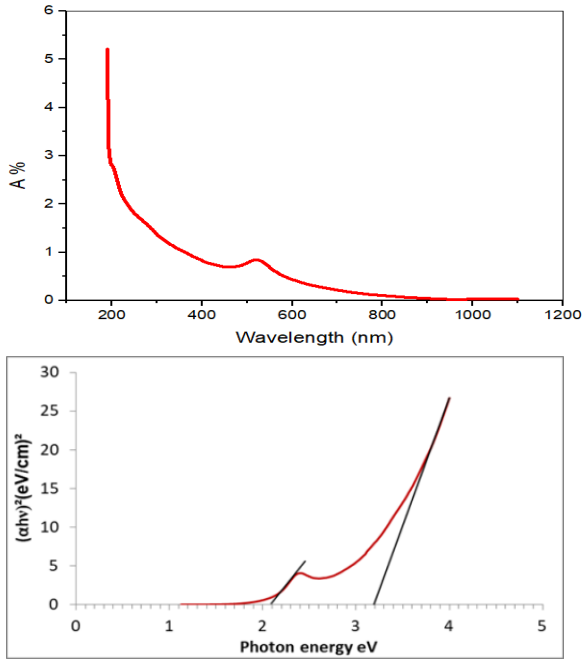

Figure 5: Absorbance and the relationship between (αhν)2 and the energy of photons curves of Fe_2O_3/Au core-shell nanoparticles.

The increased value (approximately 3.2 -3.3 eV) can be explained by inter band transitions in the gold nanoparticles or the quantum confinement effect due to the small size of the particles that was obtained by the laser scraping method [16], [17]. The laser-prepared core-shell nanoparticles of Fe_2O_3/Au, prepared on the iron oxide surface, demonstrate better optical characteristics than mono-metallic nanoparticles where deposition of the gold on the particle surface causes the generation of surface plasmonic resonance (SPR) at 520-550 nm, and makes the nanoparticles better light absorbers, and also increases the optical and biological application of such materials [18], [19].

The Fe_2O_3/Au core-shell composite nano particles have a distribution that is less than the agglomerated because of magnetic attraction between the particles that contain the iron oxide and van der Waals forces (Fig. 6) [18]. The TEM image shows the contrast of electrons in various parts of the particles and dark circles are distinctly seen in the image which is attributed to the existence of a high density of electrons in the form of gold shell around the less dense iron oxide nucleus which indicates the success of the core-shell structure [19].

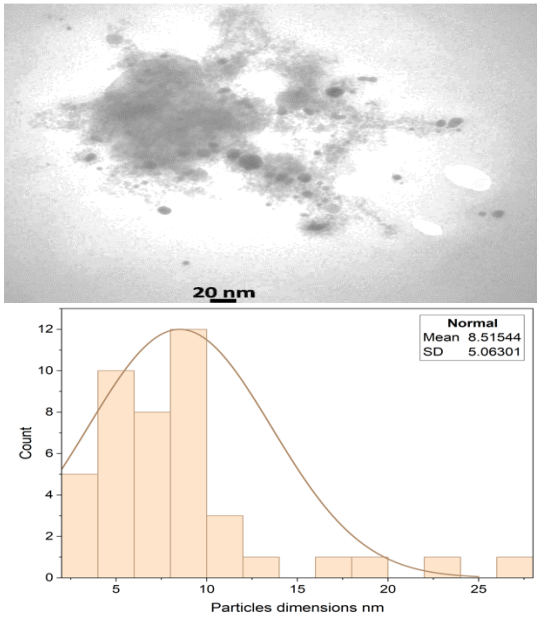

Figure 6: TEM image and particle dimensions distribution of Fe_2O_3/Au core-shell nanoparticles.

The results of the analysis of the histogram reveal that the size of the nanoparticles is about 8.52 and 5.06 nm with an average size of 8.52 and a size distribution of about 3 to 25 nm, which indicates that the production of the ultra-fine nanoparticles with a decent size distribution in accordance with the nature of the method used to produce the nanoparticles was the laser scraping technique [14]. The optical and

magnetic properties of nanoparticles formed in such manner are increased by the small size of nanoparticles which undergoes quantum effects of nanoscale confinement and increase the efficiency of surface plasmon resonance of gold and catalytic power of iron oxide [20]. The agglomeration in the microscopic picture is characteristic of the laser-prepared nanoparticles and can be minimized by altering the conditions of preparation [18], [16].

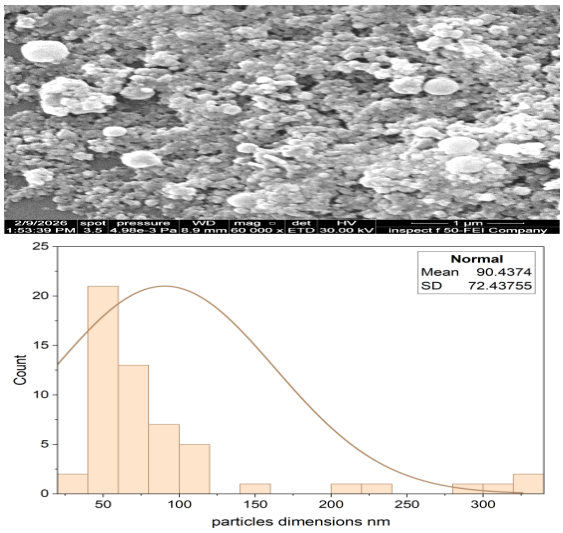

Figure 7: FESEM image and particle dimensions' distribution of Fe_2O_3/Au core-shell nanoparticles.

The Scanning Electron Microscopy (SEM) image exhibits heterogeneous structure having a large agglomerate and discrete sphericals dispersed on a fine-grained surface (Fig. 7) [18]. Massive, heavily electron-contrected spherical particles (depicted in light color), about 50-100 nm in diameter, are impregnated in a mass of lesser particles, signaling second particle fusion or deposition in the procedure of laser scraping or drying [16]. The particle size distribution histogram gives a statistical evaluation of the nanoscale dimensions, the average size of the particle is around 90.44 + 72.44 nm and the standard deviation is extremely high indicating a broad polydispersity [19]. The size difference between the primary particles (which are observed at an approximate of 8.5 nm in the earlier TEM images) and the clusters in the SEM images is confirmation of the hierarchically structure of the agglomeration in these materials with the primary nanoparticles assembling into larger clusters because of the magnetic forces of the iron oxide and van der Waals forces [20]. This large size range (nanometers to micrometers) is a typical property of laser-in-liquid scraping, in which, due to the high cooling rate and interaction of the plasma, particles of various sizes are formed simultaneously and can influence the optical and magnetic characteristics of the final composite substance eventually [18], [19].

Based on the magnetization curve (M-H) presented in the figure, the magnetic behavior of Fe_2O_3/Au core-shell nanoparticles produced by laser skimming in liquid can be characterized. The narrow symmetrical S hysteresis loop is evident and crosses the origin (Fig. 8) [21]. This property demonstrates the presence of superparamagnetism of the nanoparticles, which is a property of the iron oxides at small nanometer sizes (less than 20 nm) at room temperature [22]. Both remanent magnetization (Mr) and coercively (Hc) have very low values in the narrow loop, i.e. the particles are immediately deprived of their magnetism as soon as the external magnetic field is removed [23]. This plays an important role in biomedical applications including MRI and targeted drug delivery [24]. This large magnetic value (around 0.02 emu/g) is due to the magnetic contribution of the magnetic nucleus, which is the iron oxide (Fe_2O_3 or Fe_3O_4) and non-magnetic gold coating decreases the overall magnetic value of the pure iron oxide particles [22]. The effectiveness of laser scraping in creating particles with tremendously symmetrical magnetic characteristics and the absence of stabilizing chemicals prove the effectiveness of using this green procedure in making advanced composite nanomaterial that can be utilized in biomedical practice and magneto thermal therapy [25], [26].

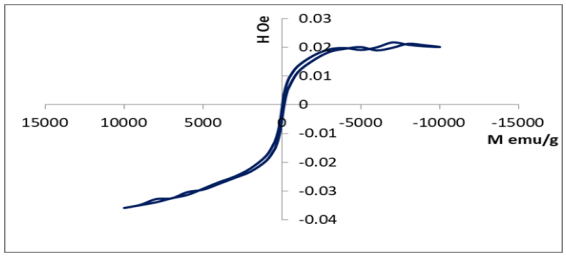

Figure 8: Magnetization curve (M-H) of Fe_2O_3/Au core-shell nanoparticles.

4 CONCLUSIONS

The success of the laser-in-liquid (PLAL) technique used in the preparation of high-purity Fe_2O_3/Au core-shell composite nanoparticles free of the presence of reducing and stabilizing reagents was demonstrated by the success of the experimental. The X-ray diffraction (XRD) revealed the presence of the face-

centered cubic (FCC) crystalline phase of gold, and the broad peaks of iron oxide indicated the nanoscale and quasi-crystalline nature of the particles, which follows due to the rapid cooling when the laser-in-liquid procedure is used. These results were further corroborated by energy-dispersive spectroscopy (EDS), which indicates the composition of the elements in the composite with most of the weight had been occupied by gold because of its greater atomic mass whereas the ratio of atoms between the two elements was more balanced. Absorption spectroscopy and Tack plots were used to demonstrate unusual hybrid materials with a combination of the characteristic surface plasmon resonance of gold between 520 550 nm and the semiconducting energy gaps of iron oxide (2.2 2.3 eV and 3.2 3.3 eV) and this has broadened the application prospects of these materials in photonic and biological applications. The results of the transmission electron microscopy (TEM) proved the achievement of the core-shell structure based on the clear electron contrast between the lighter iron oxide nucleus and the heavier gold shell with a mean elementary particle size of about 8.52 -5.06 nm. The images by scanning electron microscopy (SEM) revealed a hierarchical cluster structure through which the elementary particles combine into bigger clusters with mean size of 90.44 72.44 nm because of the magnetic and van der Waals forces, which is typical of this method. All in all, the present study is a good experimental demonstration of the effectiveness of the laser scraping technique in producing effective composite nanomaterials with enhanced optical and magnetic characteristics which can be easily tailored to the develop new applications in diagnostics, targeted therapy, and photodynamic therapy.

ACKNOWLEDGMENT

The authors would like to express their sincere gratitude to their university and college for their valuable support and assistance throughout the completion of this research.

REFERENCES

[1] M. C. Daniel and D. Astruc, “Gold nanoparticles: Assembly, supramolecular chemistry, quantum-size-related properties, and applications toward biology, catalysis, and nanotechnology,” Chem. Rev., vol. 104, no. 1, pp. 293-346, Jan. 2004, [Online]. Available: https://doi.org/10.1021/cr030698.

[2] P. Ghosh, G. Han, M. De, C. K. Kim, and V. M. Rotello, “Gold nanoparticles in delivery applications,” Adv. Drug Deliv. Rev., vol. 60, no. 11, pp. 1307-1315, Aug. 2008, [Online]. Available: https://doi.org/10.1016/j.addr.2008.03.016.

[3] K. Gupta and M. Gupta, “Synthesis and surface engineering of iron oxide nanoparticles for biomedical applications,” Biomaterials, vol. 26, no. 18, pp. 3995-4021, Jun. 2005, [Online]. Available: https://doi.org/10.1016/j.biomaterials.2004.10.012.

[4] T. T. Nguyen, F. Mammeri, and S. Ammar, “Iron Oxide and Gold Based Magneto-Plasmonic Nanostructures for Medical Applications: A Review,” Nanomaterials, vol. 8, no. 3, p. 149, 2018, [Online]. Available: https://doi.org/10.3390/nano8030149.

[5] J. Y. Zhang, M. Post, T. Veres, Z. J. Jakubek, J. Guan, D. Wang, et al., “Laser-assisted synthesis of superparamagnetic Fe@Au core-shell nanoparticles,” J. Phys. Chem. B, vol. 110, no. 14, pp. 7122-7128, Apr. 2006.

[6] S. Sun and H. Zeng, “Size-Controlled Synthesis of Magnetite Nanoparticles,” J. Am. Chem. Soc., vol. 124, no. 28, pp. 8204-8205, 2002, [Online]. Available: https://doi.org/10.1021/ja026501x.

[7] R. Basharat and M. Shaikh, “A Comprehensive Review of Gold Nanoparticles: Properties, Characterization, and Applications,” Open Journal of Physical Chemistry, vol. 16, no. 1, pp. 1-24, Feb. 2026, [Online]. Available: https://doi.org/10.4236/ojpc.2026.161001.

[8] M. Bartolomé, M. J. Villaseñor, and Á. Ríos, “Surface plasmon resonance optical sensors involving nanomaterials as reliable analytical tools: A critical view about performance and applications,” Analytica Chimica Acta, vol. 1382, Jan. 2026, [Online]. Available: https://doi.org/10.1016/j.aca.2025.344693.

[9] V. Amendola and M. Meneghetti, “Laser ablation synthesis in solution and size manipulation of noble metal nanoparticles,” Phys. Chem. Chem. Phys., vol. 11, no. 20, pp. 3805-3821, May 2009, [Online]. Available: https://doi.org/10.1039/B900654K.

[10] S. I. Dolgaev, A. V. Simakin, V. V. Voronov, G. A. Shafeev, and F. Bozon-Verduraz, “Nanoparticles produced by laser ablation of solids in liquid environment,” Appl. Surf. Sci., vol. 186, no. 1-4, pp. 546-551, Jan. 2002, [Online]. Available: https://doi.org/10.1016/S0169-4332(01)00634-1.

[11] S. Rehman, J. Kanjanawatana, and M. Horprathum, “Influence of laser parameters on the synthesis of gold nanoparticles by pulsed laser ablation in liquid,” J. Phys.: Conf. Ser., vol. 1380, no. 1, Art. no. 012068, 2019, [Online]. Available: https://doi.org/10.1088/1742-6596/1380/1/012068.

[12] S. Barcikowski and F. Mafuné, “Status and demand of research to bring laser ablation in liquids into mainstream,” J. Phys. Chem. C, vol. 115, no. 11, pp. 4985-4986, Mar. 2011, [Online]. Available: https://doi.org/10.1021/jp111036a.

[13] K. Kawaguchi, J. Jaworski, Y. Ishikawa, T. Sasaki, and N. Koshizaki, “Preparation of gold/iron-oxide composite nanoparticles by a unique laser process in water,” J. Magn. Magn. Mater., vol. 310, no. 2, pp. 2369-2371, Mar. 2007, [Online]. Available: https://doi.org/10.1016/j.jmmm.2006.11.109.

[14] Świątkowska-Warkocka, K. Kawaguchi, Y. Wang, T. Koshizaki, and N. Koshizaki, "Spectroscopic and Microscopic Analyses of Fe_3O_4/Au Nanoparticles Prepared by Laser Ablation in Liquid for Surface-Enhanced Raman Scattering Applications," Materials, vol. 13, no. 4, 2020, [Online]. Available: https://doi.org/10.3390/ma13040986.

[15] M. J. Rivera-Chaverra, E. Restrepo-Parra, C. D. Acosta-Medina, A. Mello, and R. Ospina, "Synthesis of oxide iron nanoparticles using laser ablation for possible hyperthermia applications," Nanomaterials, vol. 10, no. 11, Art. no. 2099, Nov. 2020, [Online]. Available: https://doi.org/10.3390/nano10112099.

[16] H. S. Mahmood and N. F. Habubi, "Preparation of samarium doped-PMMA composite by casting method to evaluate the optical properties and potential applications," J. Optoelectron. Adv. Mater., vol. 25, no. 2, pp. 56-61, 2023.

[17] S. Idrissi, A. Lahmar, M. E. Sanad, and L. Bahmad, "Analysis and characterization of opto-electronic properties of iron oxide nanoparticles for optoelectronic applications," J. Mater. Res. Technol., vol. 24, pp. 7896-7908, May-Jun. 2023, [Online]. Available: https://doi.org/10.1016/j.jmrt.2023.06.171.

[18] A. Akouibaa, R. Masrour, A. Jabar, M. Benhamou, and A. Derouiche, "Optical and dielectric properties of plasmonic core-shell nanoparticles: Fe_2O_3/Au and Fe_3O_4/Au," J. Cluster Sci., vol. 33, no. 5, pp. 2139-2146, Sep. 2022, [Online]. Available: https://doi.org/10.1007/s10876-021-02133-1.

[19] H. A. Alrubaie and R. Salam, "Optical and structural properties of Au@Fe_2O_3 nanoparticles synthesized by nanosecond laser ablation in liquid," Semiconductors, vol. 59, no. 5, pp. 436-440, May 2025, [Online]. Available: https://doi.org/10.1134/S1063782625600019.

[20] M. Muniz-Miranda, F. Muniz-Miranda, and E. Giorgetti, "Spectroscopic and Microscopic Analyses of Fe_3O_4/Au Nanoparticles Obtained by Laser Ablation in Water," Nanomaterials, vol. 10, no. 1, Art. no. 132, 2020, [Online]. Available: https://doi.org/10.3390/nano10010132.

[21] M. Mahmoudi, A. Simchi, M. Imani, and U. O. Häfeli, "Superparamagnetic Iron Oxide Nanoparticles with Rigid Cross-Linked Polyethylene Glycol Fumarate Coating for Application in Imaging and Drug Delivery," J. Phys. Chem. C, vol. 113, no. 19, pp. 8124-8131, 2009, [Online]. Available: https://doi.org/10.1021/jp810771m.

[22] M. Mahmoudi, S. Sant, B. Wang, S. Laurent, and T. Sen, "Superparamagnetic iron oxide nanoparticles (SPIONs): Development, surface modification and applications in chemotherapy," Adv. Drug Deliv. Rev., vol. 63, no. 1-2, pp. 24-46, Jan. 2011, [Online]. Available: https://doi.org/10.1016/j.addr.2010.05.006.

[23] A. Tymoczko, M. Kamp, C. Rehbock, L. Kienle, E. Cattaruzza, S. Barcikowski, and V. Amendola, "One-Step Synthesis of Fe-Au Core-Shell Magnetic-Plasmonic Nanoparticles Driven by Interface Energy Minimization," Nanoscale Horizons, vol. 4, no. 6, pp. 1326-1332, 2019, [Online]. Available: https://doi.org/10.1039/C9NH00332K.

[24] M. Colombo, S. Carregal-Romero, M. F. Casula, L. Gutiérrez, M. P. Morales, I. B. Böhm, et al., "Biological applications of magnetic nanoparticles," Chem. Soc. Rev., vol. 41, no. 11, pp. 4306-4334, Jun. 2012, [Online]. Available: https://doi.org/10.1039/C2CS15337H.

[25] S. Barcikowski and G. Compagnini, "Advanced Synthesis and Processing of Colloids by Laser Ablation," Phys. Chem. Chem. Phys., vol. 15, no. 9, pp. 3022-3026, 2013, [Online]. Available: https://doi.org/10.1039/C3CP43802H.

[26] H. H. Ahmed, T. A. Mezher, and M. R. Rashid, "Laser-Ablated CdS and Ag_2O Nanomaterials for High-Sensitivity Photodetectors," Chal. Lett., vol. 22, no. 12, pp. 1055-1066, Dec. 2025, [Online]. Available: https://doi.org/10.15251/CL.2025.2212.1055.